

A proteoglycan that activates fibroblast growth factors during early neuronal development is a perlecan variant

Sharon J. Joseph¹, Miriam D. Ford¹, Christian Barth², Stuart Portbury¹, Perry F. Bartlett³, Victor Nurcombe^{1,*} and Ursula Greferath¹

¹Department of Anatomy and Cell Biology, University of Melbourne, Parkville, 3052, Australia

²Department of Microbiology, LaTrobe University, Bundoora, 3083, Australia

³Walter and Eliza Hall Institute for Medical Research, Royal Melbourne Hospital, Parkville 3050, Australia

*Author for correspondence (e-mail: nurcombe@vesalius.anatomy.unimelb.edu.au)

SUMMARY

Cells in the early embryonic vertebrate nervous system are dependent on members of the fibroblast growth factor (FGF) family for their proliferation and subsequent differentiation. These growth factors will only bind to their specific high affinity cell surface receptors after formation of a ternary complex with the glycosaminoglycan heparan sulfate. Such specific heparan sulfates are secreted as proteoglycans from neural precursor cells and localise to their surfaces. One such proteoglycan, HSPG-PRM (Perlecan-related molecule), was isolated through its ability to potentiate neural cell responses to either FGF-1 or FGF-2. In this study, we have verified the relative molecular mass of the core protein of PRM as 45,000 and obtained partial amino acid sequence from it. The sequences bore significant homology to native perlecan. A probe generated by reverse transcriptase polymerase chain reaction using oligonucleotides designed from the protein sequence used on northern blots of RNA from a neuroepithelial cell line detected perlecan at 12.6 kilobases, as well as novel transcripts at 6.5 and 3.5 kilobases. The latter species appears

by virtue of its size and abundance to be the novel PRM transcript. PRM appears to be encoded by the same gene as perlecan, as genomic Southern blotting only detected a single gene. Polyclonal antibodies raised against the PRM molecule detected a single proteoglycan species at 290×10^3 with a core protein of 45×10^3 . Polyclonal anti-perlecan antibodies cross-reacted with PRM confirming their relatedness, although immunohistochemical studies revealed a differential staining pattern for PRM as compared to perlecan within the developing nervous system. The PRM molecule was shown to be localised to several different tissues of the developing embryo, indicating that it plays a broad role. We conclude that PRM is a variant of perlecan that is differentially glycosylated in a manner that confers highly specific functions at critical stages of neural development and tissue growth.

Key words: perlecan, heparan sulfate proteoglycan, fibroblast growth factor, neuroepithelium

INTRODUCTION

Heparan sulfate proteoglycans (HSPGs) are a class of macromolecules that consist of a protein core to which heparan sulfate (HS) glycosaminoglycan side chains are covalently attached (Gallagher and Turnbull, 1992). There are essentially three broad classes of HSPG: (1) those that are secreted by cells and located in the extracellular matrix (ECM); (2) those associated with the cell membrane and (3) the transmembrane forms. A prototypical matrix HSPG is the large basement membrane proteoglycan perlecan, initially isolated from the murine Engelbreth-Holm-Swarm (EHS) tumour (Hassell et al., 1980). Transmembrane HSPGs include the syndecans, of which there are four members (Saunders et al., 1989). The cell-associated species include the glypicans, which have a GPI anchor (David, 1991). Over the past few years it has been recognised that HSPGs are not just structural elements, but amongst other functions are able to bind and sequester essential growth factors. For example, perlecan has recently been shown

to bind to FGF-2 (Aviezer et al., 1994). They thus play critical roles in cell growth, migration and differentiation (Wight et al., 1992; Ruoslahti and Yamaguchi, 1991; Kjellen and Lindahl, 1991).

Perlecan is one of the largest gene products known, with a core protein over 400 kDa ($\times 10^3 M_r$) in size (Iozzo and Hassell, 1989; Noonan et al., 1991). It is a complex molecule composed of five structural domains (Iozzo et al., 1994). Domain 1 is unique to perlecan and is the site to which three heparan sulfate side chains are attached. Other domains contain peptide sequence repeats, with domains homologous to the LDL receptor, laminin, N-CAM and EGF. Domain IV is the largest, containing several immunoglobulin repeats homologous to N-CAM. This domain shows the greatest differences between human and mouse, as the human form contains 21 instead of 14 repeats. There is some evidence for mouse cDNAs containing extra repeats in this region, indicating the possibility of alternative splicing of mRNA (Noonan and Hassell, 1993). The complex multidomain structure of perlecan clearly suggests

that it has the potential for diverse function (Murdoch and Iozzo, 1993). The purported roles of perlecan are numerous and include interactions with other ECM molecules such as fibronectin, various collagens and laminin (Yurchenco and Schittny, 1990), and with itself (Yurchenco et al., 1987). Perlecan has been implicated in such human pathologies as diabetes (Rohrbach et al., 1982, 1983), Alzheimer's Disease (Snow et al., 1989) and tumour progression (Iozzo and Wight, 1982).

HSPGs bind FGFs through their heparan sulfate side chains. Specific FGF-2-binding sites on heparan sulfate chains derived from fibroblasts have been shown to contain defined carbohydrate sequences (Gallagher and Turnbull, 1992). It appears that HSPGs act to deliver FGFs to their high affinity cell surface receptors, which are then activated after formation of ternary complexes (Kan et al., 1993; Wang et al., 1995). More recently, a novel HSPG called PRM (perlecan-related molecule) has been isolated from embryonic mouse neuroepithelial cells and the 2.3D cell line and shown to differentially bind FGF-2 and FGF-1 at defined stages of early neural development (Nurcombe et al., 1993). During the periods of most active mitogenesis, PRM binds FGF-2. At embryonic day (E11), the core protein of PRM becomes differentially glycosylated, so switching affinity to FGF-1, which is expressed just as neuronal differentiation begins. The core protein of PRM remains unchanged over both stages of development.

The present study was directed towards further characterising the HSPG-PRM molecule. Limited amino acid sequencing of the core protein revealed homology to perlecan and led to the identification of a highly abundant 3.5 kb mRNA transcript. Hence, this study confirms the existence of mRNA and protein perlecan variants in higher vertebrates. Genomic Southern blotting demonstrated that only one gene encodes the variant perlecan forms. Although polyclonal antibodies to native perlecan showed cross-reactivity with HSPG-PRM, antibodies specific to the PRM molecule revealed a unique immunohistochemical staining pattern within the developing neuroepithelium. This study therefore demonstrates that a novel perlecan variant, capable of varying binding capacities for specific growth factors, is present within the nervous system, and other tissues, at stages when key proliferative and differentiative events are occurring.

MATERIALS AND METHODS

Protein sequencing

In order to generate fragments of the PRM proteoglycan core proteins for NH₂-terminal amino acid sequencing, HSPG fractions from medium conditioned by the 2.3D neuroepithelial cell line were taken after anionic exchange and gel filtration chromatography and subjected to heparitinase (ICN; 50 units/mg) and chondroitinase ABC (Sigma; 10 units/ μ g) digestion (both for 16 hours at 37°C in 100 mM Tris, pH 7.2) to remove the carbohydrate, repurified over hydroxyapatite and then digested with either trypsin or with V8 protease essentially according to the method of Noonan et al. (1988).

Polymerase chain reaction (PCR), generation and labelling of cDNA probes

For RT-PCR, the forward primer (HSPG-1) : GGTGCTAGCTGTGAACAG and reverse primer (HSPG-2): CCATGCTACGGAGCCCT, were designed to peptides homologous to mouse perlecan with

the respective amino acid coordinates 1134-9 and 1160-65 (Noonan et al., 1991). RT-PCR was carried out using the RNA PCR kit (Perkin-Elmer Cetus) conducted with 100 ng poly(A)⁺ RNA isolated from the 2.3D cell line. The 96 base pair product generated was subcloned into PCR-script vector (Stratagene) and nucleotide sequence was verified using FmolTM DNA sequencing system (Promega). This PCR-generated 96 bp, cDNA clone was designated PERL-1 and was used as a probe for northern and genomic Southern analysis. The PERL-1 clones containing the 96 bp inserts were end-filled labelled with [α -³²P]dCTP as the labelling nucleotide using the standard random priming procedure, except that HSPG-1 and HSPG-2 PCR primers were used to produce probes with very high levels of specific activity. The 1.2 kb mouse perlecan cDNA probe was isolated from a mouse embryonic day 11.5 gt11 library (Clontech). It was derived from domain 3 and includes the 96 bp region. It was labelled using standard random priming methodologies.

Northern blot analysis

Approximately 10 μ g of poly(A)⁺ RNA isolated from the 2.3D cell line was electrophoresed through a 1.2% agarose-formaldehyde gel and blotted onto Hybond N-CAM (Amersham) membrane by alkaline blotting. After prehybridization at 68°C for 2 hours in 6 \times saline-sodium citrate (SSC) buffer, 5 \times Denhardt's solution, 100 μ g/ml salmon sperm DNA and 0.1% SDS, hybridisation was carried out at 68°C for 15 hours in the same buffer with the addition of α -³²P-labeled cDNA probe. Blots were washed twice in 2 \times SSC and 0.1% SDS for 10 minutes at room temperature. The stringency of the final wash was 68°C with 0.1 \times SSC and 1% SDS for 15 minutes. The blots were exposed at -70°C for 4 days to Kodak XAR-5 X-ray film with one intensifying screen. Analysis of the northern blot was performed on a Phosphor Imager (Fujix BAS 1000) and numerical values for band intensities obtained. Variant mRNA species were quantified by expressing the intensity of the mRNA variants as a relative percentage to the most abundant mRNA variant (3.5 kb).

Southern blot analysis

Genomic DNA was isolated from the 2.3D cell line and analysed by pulsed-field gel electrophoresis (PFGE). Cells were washed in PBS and mixed with an equal volume of 1% InCert agarose (FMC Bio-products) prepared in PBS and cooled to 39°C. The final cell concentration was 1.5 \times 10⁷ cells/ml. After casting the aliquots, the solidified agarose plugs (~30 μ l volume containing 5 \times 10⁵ cells) were incubated in digestion buffer (0.5 M EDTA, pH 8.0; 2% sodium lauroyl-sarcosinate; 2 mg/ml Proteinase K) for 48 hours at 50°C. For restriction enzyme digestion, the agarose plugs were repeatedly washed in TE (the first washes containing 1 mM phenylmethylsulfonyl fluoride) and incubated overnight at 37°C in 50-100 U of restriction enzyme. PFGE was performed using a CHEF apparatus (contour-clamped homogenous electric fields, Biorad) (Chu et al., 1986). CHEF gels were 1% agarose in 0.5 \times TBE running buffer. The single digested plugs were loaded in the gel. PFGE was for 10 hours, 5-10 seconds switching time at 200 V and 14°C. Agarose gels were stained with ethidium bromide and photographed. Southern transfer was by acid depurination (0.25 M HCl) and alkaline transfer (0.4 M NaOH, 1.5 M NaCl) to Hybond N-CAM membrane (Amersham). After prehybridization at 50°C for 2 hours in 5 \times saline-sodium citrate (SSC) buffer, 5 \times Denhardt's solution, 200 μ g/ml salmon sperm DNA and 0.1% SDS, hybridisation was carried out at 50°C for 15 hours in the same buffer containing 15% formamide with the addition of α -³²P-labeled cDNA probe. Blots were washed twice in 2 \times SSC and 0.1% SDS for 10 minutes at room temperature. The stringency of the final wash was 50°C with 0.1 \times SSC and 1% SDS for 30 minutes. Blots were analysed on a Phosphor Imager (Fujix BAS 1000).

Purification of proteoglycans and analysis of core proteins

Conditioned media from the 2.3D mouse neuroepithelial cell line was

subjected to anion exchange chromatography over DEAE Sephadex columns, and eluted fractions desalted and concentrated using membrane cones (CF 25-25,000 M_r ; Amicon) spun at 3000 g . In order to obtain a profile of the 2.3D cell line conditioned medium, aliquots of the isolated proteins were run on 7% sodium dodecyl sulfate-polyacrylamide (SDS-PAGE) gels and visualised by silver staining (Biorad). Isolated protein fractions were subsequently used for immunoprecipitation and western blotting. To class and size the PRM-core protein, 2.3D proteoglycan aliquots were digested with heparanase III lyase (Sigma). Digestion involved 0.25 U of the enzyme in buffer (500 mM sodium acetate, 0.5 mM calcium acetate, pH 7), at 37°C for 15 hours. The digested protein samples were electrophoresed on 15% SDS-PAGE gels and visualised with appropriate antibodies.

Immunoprecipitation

Aliquots of 2.3D proteoglycan core protein preparations (20 μ l, containing approximately 20 μ g) were added to 800 μ l of immunoprecipitation buffer (50 mM Tris-HCl, pH 7.8, 150 mM NaCl, 1% Triton X-100, 2 mM *N*-ethylmaleimide, 2 mM PMSF). 100 μ l of *Staphylococcus aureus* suspension (10% in the immunoprecipitation buffer; Pansorbin, Calbiochem Frankfurt). After preabsorption for 1 hour at room temperature, the beads were removed by centrifugation and 10 μ g of anti-EHS perlecan polyclonal antibodies (a gift of Dr Marie Dziadek, University of Melbourne) added to the supernatant. After overnight incubation at 4°C, 50 μ l of the Pansorbin suspension was added for a further 1 hour. The Pansorbin beads were then washed three times with PBS. Laemmli sample buffer (40 μ l of Tris-glycine, pH 8.5 with 2-mercaptoethanol) was added to the beads, which were then boiled for 10 minutes prior to SDS-PAGE electrophoresis.

Immunoblotting

Following SDS-PAGE, proteoglycans were transferred to Immobilon-P membranes (Millipore) with an electroblotter (Biorad; 200 V for 1 hour). The membranes were blocked with Tween-20/Tris-buffered saline (TTBS) for 1 hour, and then incubated with one of the following primary antibodies: polyclonal PRM-HSPG (Nurcombe et al., 1993) used at 1:1,000; rabbit anti-perlecan antibodies, used at 1:1,000, or anti-perlecan rat monoclonal antibodies (Upstate Biotechnology) used at 5 μ g/ml. The blots were washed three times in TTBS for 15 minutes intervals and then incubated with an alkaline phosphatase-conjugate secondary antibody (anti-rabbit IgG, 1:1,000 dilution). They were then washed in TTBS as previously, and developed with 60mg of naphthol (N-5000) ASMX phosphatase diluted in H₂O, and mixed with fast red F-1500 (Sigma) diluted in alkaline phosphatase buffer (Tris 0.2 M, MgCl₂ 5 mM, pH 8) to visualise immunoreactive bands.

Immunohistochemistry

Whole mouse embryos (E9, E10, E12, E16) were fixed for 1 hour (E9, E10, E12) or overnight (E16) in 4% paraformaldehyde (PFA), washed in PBS and immersed in 30% sucrose overnight. Transverse sections (12-18 μ m) were cut on a cryostat, collected on gelatin-coated slides and stored at -70°C. Details of the immunohistochemical methods used are given elsewhere (Greferath et al., 1990). The rabbit polyclonal antibody directed against HSPG-PRM (Nurcombe et al., 1993) was used at 1:100 and the rat monoclonal antibody against perlecan was used at 1:10. Immunoreactivity was demonstrated using either carboxymethylindocyanine (Cy3)-coupled secondary antibodies (goat anti-rabbit-, goat anti-mouse-Cy3; Medical Dynamics, Australia) were used at 1:1000 in PBS, or fluorescein isothiocyanate (FITC)-coupled secondary antibodies (goat anti-rabbit-, goat anti-rat-FITC, Sigma, Australia) used at 1:100.

In double-labelling studies, cryostat sections were incubated in a mixture of the primary antibodies and subsequently in a mixture of the secondary antibodies. To control cross-reactivity of the secondary antibodies, double immunofluorescence staining was performed by omitting one of the primary antisera. In order to localise the rat mon-

oclonal antibody specific to perlecan, anti-mouse-Cy3 secondary antibody was often used instead of anti-rat secondary antibodies. This was possible because of a high cross-reactivity of the anti-mouse Cy3 antibody. A close comparison of the perlecan specific staining using anti-mouse-Cy3 or anti-rat-FITC in adjacent sections demonstrated that the staining was identical.

RESULTS

Northern blot analysis

Northern blot analysis was performed with the 96 bp PERL-1 PCR product to identify mRNA transcripts in the 2.3D neuroepithelial cell line. The expected 12.6 kb mRNA transcript of perlecan was detected, as well as two other, smaller variants at 6.5 kb and 3.5 kb (Fig. 1A). Quantitative analysis of the three mRNA species using phosphor imaging indicated that the 3.5kb mRNA transcript was the most abundantly expressed species, at levels tenfold higher than that of perlecan. The 6.5 kb mRNA transcript was detected at approximately one quarter the level of the 3.5 kb transcript. The relatively high abundance of the 3.5 kb mRNA species suggests that it is the putative HSPG-PRM mRNA, as it is the expected size to encode a protein of 45 kDa. Syndecan-1 and Syndecan-3 mRNA were also detected in the 2.3D cell line (Fig. 1B). The expected 3.4 kb and 2.6 kb polyadenylation variants of syndecan-1 (Vihinen et al., 1993) were identified. A syndecan-3 cDNA probe hybridised to a 5.6 kb species (Carey et al., 1992.) and an unknown variant of 3.4 kb (Fig. 1C). Quantitative analysis confirmed that the most abundant HSPG mRNA transcript in the 2.3D cell line appeared to be the 3.5 kb putative PRM species.

Southern blot analysis

The different mRNA variants could be the product of alternative splicing of the perlecan gene, or of a related but separate gene. To address this question, Southern blot analysis was

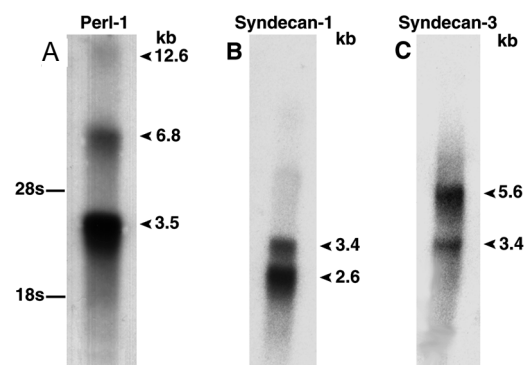


Fig. 1. (A) Northern blot analysis of poly(A)⁺ RNA isolated from the mouse 2.3D neuroepithelial cell line. 10 μ g of poly(A)⁺ RNA was probed at high stringency with the 96 bp cDNA probe. The expected 12.6 kb mRNA transcript of perlecan was detected, as well as two other smaller variants at 6.5 kb and the highly abundant putative PRM species of 3.5 kb. (B) The blot was reprobed with a syndecan-1 cDNA probe, which detected the expected 3.4 kb and 2.6 kb polyadenylation variants. (C) A syndecan-3 cDNA probe hybridised to 5.6 kb and 3.4 kb transcripts in the 2.3D cell line. The bars on the left indicate the positions of the 28S and 18S ribosomal RNA.

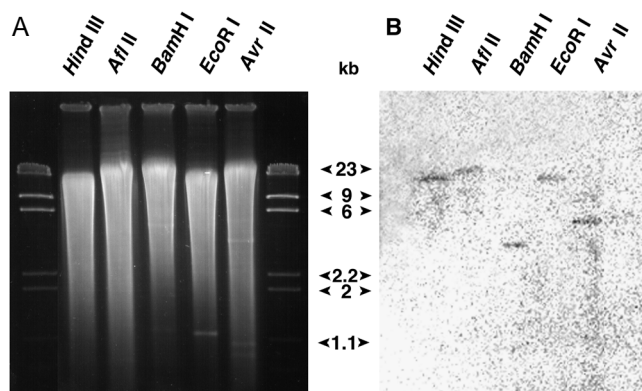


Fig. 2. Southern blot analysis of 2.3D genomic DNA (DNA of 5×10^5 cells/well) which was digested with *Hind*III, *Afl*II, *Bam*HI, *Eco*RI or *Avr*II and separated by PFGE as described in Materials and Methods. Ethidium-bromide-stained agarose gels were photographed (A), blotted and hybridized with the 96 bp cDNA probe (B). Only a single band could be detected in the different digests. *Hind*III-digested λ size standards are indicated in kilobases.

performed with the 96 bp PERL-1 probe. Genomic DNA of the 2.3D cell line was prepared in agarose plugs to prevent mechanical damage, and then digested with a variety of restriction enzymes with 6-base pair recognition sites that do not cut within the 96 bp region. The digests were separated by PFGE under conditions that allow optimal separation of the generated DNA fragments (Fig. 2A). Only a single band could be detected in the various digests, demonstrating that there is only a single gene containing the 96 bp sequence (Fig. 2B). The blot was re-probed with a 1.2 kb mouse perlecan cDNA probe derived from domain 3 with identical results, which confirms that the 96 bp fragment was derived from perlecan and not some closely related gene (results not shown).

Immunoblotting of proteoglycans

Anion exchange chromatography of proteoglycans from 2.3D cell conditioned medium indicated the presence of at least

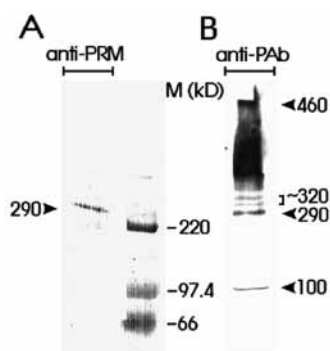


Fig. 3. Immunoblots of proteoglycans obtained from 2.3D-conditioned medium and isolated by anion exchange chromatography. (A) Blot using anti-PRM polyclonal antibody which detected a single band corresponding to 290 kDa. (B) Polyclonal antibodies to perlecan (anti-PAb) detected the native species of 460 kDa, as well as at least four other isoforms, including the 290 kDa PRM molecule. The size of molecular weight standards (M) is shown in kDa.

eight protein species ranging from approximately 40 to over 400 kDa (data not shown). This protein extract was western blotted, and polyclonal anti-PRM antibodies used to detect a single band at 290 kDa (Fig. 3A). In contrast, polyclonal antibodies against perlecan (anti-PAb) detected the expected native species of 400 kDa, as well as four other isoforms, including the 290 kDa PRM molecule (Fig. 3B). The polyclonal perlecan antibodies thus appear to cross-react with PRM, although the PRM polyclonal antibodies did not cross-react with native perlecan, or any of its variant forms from the 2.3D cell line. Specific monoclonal antibodies failed to detect syndecan-1 in the 2.3D cell media.

Immunoblot analyses of 2.3D proteoglycans and core proteins

2.3D conditioned medium fractions were treated with heparanase III to generate HSPG core proteins. Treatment with lyase resulted in the generation of a highly abundant core protein of 45 kDa, although the existence of less abundant core proteins was confirmed by silver staining (Fig. 4A). A monoclonal anti-perlecan antibody (mAb) used for analysis of the heparanase III-treated sample revealed specific reactivity (in red) to the native perlecan core protein of 400 kDa and a variant of 58 kDa. The antibody did not appear to cross-react with the 45 kDa core protein of PRM, which had transferred to the blot heavily, apparent as yellow background (Fig. 4B). A polyclonal anti-perlecan antibody reacted with the native perlecan core protein of 400 kDa, as well as with three other variants, including the 58 kDa species and the 45 kDa core protein of PRM, which had all been immunoprecipitated with the anti-perlecan antibody (Fig. 5C). Interestingly, neither the monoclonal nor the polyclonal anti-perlecan antibodies were able to completely immunoprecipitate the FGF-2 promoting activity of the 2.3D conditioned medium, unlike the anti-PRM

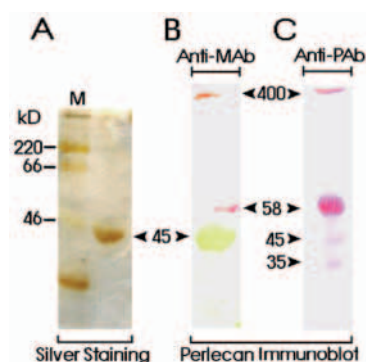


Fig. 4. Immunoblots of 2.3D conditioned medium protein samples treated with heparanase III to reveal HSPG core proteins. (A) Silver staining of a lyase-treated proteoglycan sample from 2.3D cell medium reveals the major core protein species of PRM at 45 kDa; less abundant core proteins are also present. (B) Immunoblot using anti-perlecan monoclonal antibody (mAb) revealed reactivity to the native perlecan core protein of 400 kDa and a variant of 58 kDa. The monoclonal antibody did not appear to cross-react with the 45 kDa core protein of PRM. (C) Immunoblot of immunoprecipitated protein sample using polyclonal antibodies to perlecan (anti-PAb) indicated reactivity with the native perlecan core protein of ~400 kDa, as well as three other variants, including the 58 kDa species and the 45 kDa core protein of PRM. The size of molecular weight standards (M) is given in kDa.

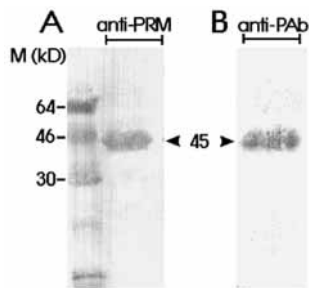


Fig. 5. Immunoblot analyses of a purified sample of the 45 kDa core protein of PRM. (A) Immunoblot using anti-PRM polyclonal antibody revealed reduced reactivity to the 45 kDa core protein as compared to the intact 290 kDa parent molecule. (B) The anti-perlecan polyclonal antibody (PAb) was also found to partially cross-react with the 45 kDa core protein of PRM. The size of molecular weight standards (M) is given in kDa.

antibodies (data not shown). A purified sample of the 45 kDa PRM core protein was used in subsequent western blot analyses. The anti-PRM-specific polyclonal antibody did not appear to bind as strongly to the isolated core protein as it had with the intact 290 kDa molecule under similar conditions (Fig. 5A). The anti-perlecan polyclonal antibody was also found to partially cross-react with the PRM core protein (Fig. 5B).

Localisation of PRM and perlecan in E10 and E16 neural tissue

The expression pattern of PRM and perlecan was examined by immunohistochemical double labelling of E10 mouse cryostat sections. The PRM-specific polyclonal antibody could be localised around individual neuroepithelial cells, as well as in

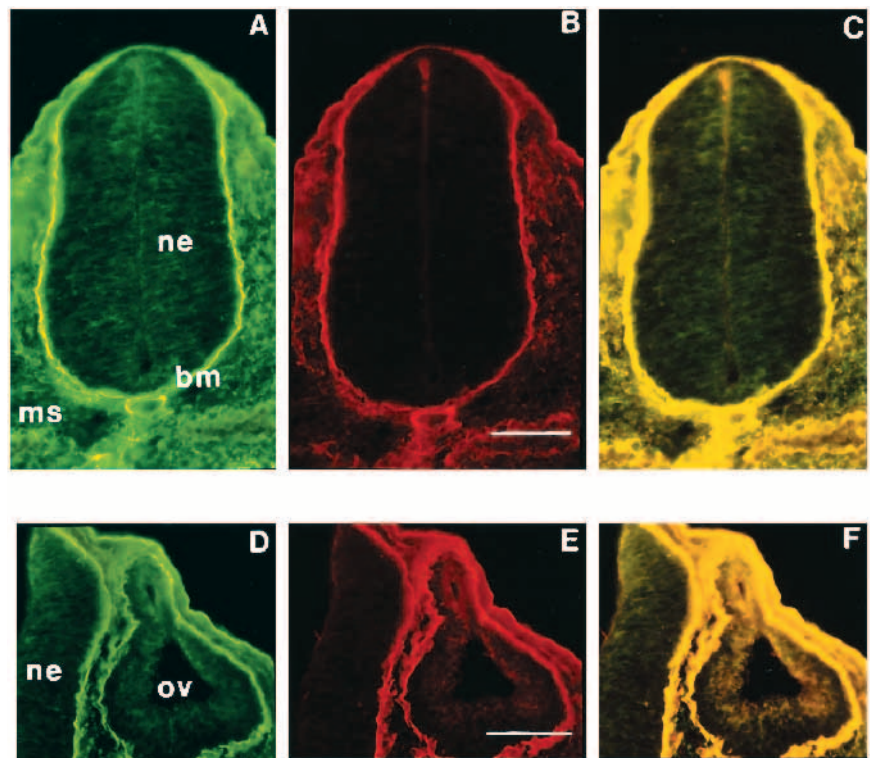
the basement membrane and mesoderm surrounding the spinal cord (Fig. 6A). In contrast, double labelling with the monoclonal anti-perlecan antibody colocalised with PRM only to the basement membrane and the mesoderm. Perlecan immunoreactivity was not detectable in or around the neuroepithelial cells (Fig. 6B). Superimposition of both staining patterns clearly demonstrates the unique expression of PRM in the neuroepithelium of the developing spinal cord (Fig. 6C). This unique expression of PRM was observed in neuroepithelial cells throughout the entire neural tube (Fig. 6D), as well as in the optic vesicle (data not shown). Interestingly, it was observed that neural precursor cells of the placodally derived otic vesicle appear to express both PRM and perlecan (Fig. 6D-F).

Differential staining for PRM and perlecan was also observed in embryonic neural tissue sections at E16.5. At this developmental stage, the remaining neural precursor cells lining the inner face of the ventricular zone of the third ventricle (Fig. 7A) and the lateral ventricle (Fig. 7C) continued to express PRM. In contrast, perlecan immunoreactivity was absent in these regions (Fig. 7B,D). Both antibodies labelled the endothelial cells of blood vessels.

Localisation of PRM during embryonic neural tissue development

Transverse sections of spinal cord from high cervical levels of E9, E10, E12 and E16 mouse embryos were stained with the PRM-specific polyclonal antibodies. PRM was localised around individual neuroepithelial cells at E9 and E10. The neuroepithelial cells close to the lumen of the neural tube appeared to be more intensely stained. The basement membrane and mesoderm surrounding the spinal cord are also intensely stained. (Fig. 8A,B). Interestingly, analysis of E9 spinal cord revealed strong staining of the floor plate cells (Fig. 8A).

Fig. 6. Micrographs of horizontal sections through an E10 mouse embryo. Sections were double immunostained for PRM, visible in green (FITC) fluorescence (A,D) and perlecan, visible in red (Cy3) fluorescence (B,E). Stains were superimposed (yellow) to visualise colocalisation (C,F). Scale bar, 100 μ m. (A-C) Section through the spinal cord. (A) PRM immunoreactivity is localised to the basement membrane (bm), the mesoderm (m) and around individual neuroepithelial cells in the neuroepithelium (nep). (B) Perlecan is localised to basement membrane and mesoderm but not to the neuroepithelial cells. (C) Superimposition of A and B demonstrates colocalisation of PRM and Perlecan immunoreactivity in the basement membrane and mesoderm. PRM is uniquely found in the neuroepithelium. (D-E) Section through the head region at the level of the otic vesicle. (D) PRM immunoreactivity is localised to neural precursor cells of the otic vesicle (ov) and the neural tube. (E) Perlecan is localised to precursor cells of the otic vesicle, but not the neural tube. (F) Superimposition of D and E demonstrates colocalisation of PRM and Perlecan in the otic vesicle and unique PRM expression in the neural tube.



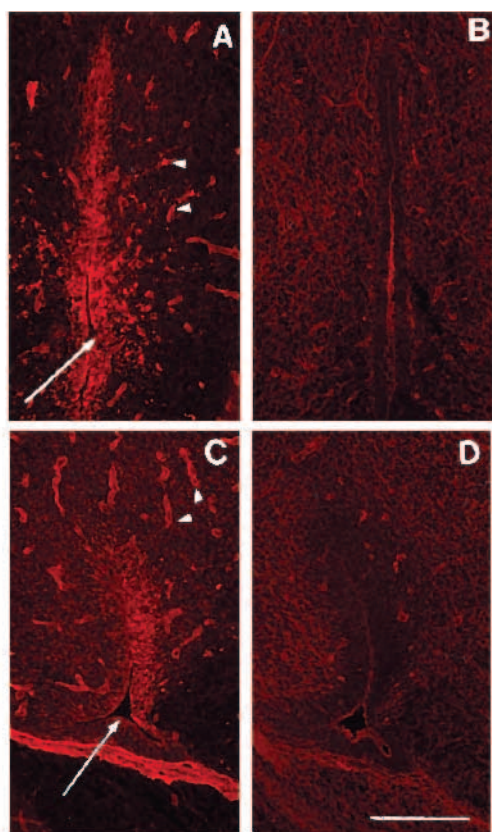


Fig. 7. Micrographs of horizontal sections through the head of an E16.5 mouse embryo. Sections in A and C were immunostained for PRM; sections in B and D, which are adjacent to A and B, respectively, were stained for perlecan. Neuroepithelial cells lining the inner face of the ventricular zone of the third ventricle (A) and the lateral ventricle (C) show PRM immunoreactivity, but are not stained by the anti-perlecan antibody (B,D). Arrows point to the ventricular lumen; arrowheads indicate labelled blood vessels in the neuroepithelium. Scale bar, 100 μ m.

Slightly later in development, at E12, PRM revealed a pattern of staining restricted to the diminishing population of precursor (dividing) cells lining the central canal of the spinal cord (Fig. 8C). Blood vessels within the spinal cord and the surrounding basement membrane and mesoderm were also stained. A transverse section of E16 spinal cord also revealed staining of the remaining neural precursor cells which line the central canal (Fig. 8E,F). The dorsal root ganglia (DRG) surrounding the spinal cord stained very intensely, as did the basement membrane and surrounding mesoderm. Examination of the staining pattern in the olfactory region of the embryo at E16 was also interesting as anti-PRM antibodies stained the ECM intensely. Within the olfactory epithelium, the staining pattern for PRM revealed long strands of immunoreactivity, which appeared to extend from the underlying basement membrane towards the epithelial surface (Fig. 9).

Localisation of PRM in the whole embryo

Sagittal sections of a whole E10 mouse embryo were also stained with the PRM-specific polyclonal antibody. PRM was heavily localised to the ECM and basement membrane of various tissues of the E10 embryo, as well as staining mes-

enchyme and ectoderm (Fig. 10). Staining was apparent in the basement membrane and neuroepithelium of the mesencephalon and the fourth ventricle, although staining of individual cells could not be visualised at this magnification. The somites of the spinal cord are also stained, particularly towards their dorsal aspect, and may reflect the ingrowth of sensory fibres from the dorsal root ganglia. The tail region also revealed strong PRM staining in the neuroepithelial cells of the neural lumen. The eye capsule stained intensely, as did the basement membranes and mesenchyme of the forelimb, lung bud and gut. PRM is also heavily localised to the vascular system, especially the heart.

DISCUSSION

The aim of the experiments described in this paper was to further characterise PRM, a novel HSPG involved in growth factor regulation during early neural development. Overall, the results from this study demonstrate the existence of a perlecan splice variant with a unique distribution. Limited amino acid sequencing of this molecule revealed homology to perlecan. A 96 bp PCR product, homologous to both PRM and perlecan, identified three mRNA species in the 2.3D cell line: the expected 12.6 kb species of perlecan (Iozzo and Hassell, 1989), and two novel variants: a 6.5 kb transcript and a highly abundant 3.5 kb transcript. The latter species we believe to be the putative PRM transcript due to its abundance and size, which is sufficient to encode a 45 kDa protein. This study confirms the existence of smaller mRNA perlecan splice variants as to date there have been reports only of larger perlecan mRNA variants in the mouse (Noonan et al., 1991). Mouse perlecan is smaller than the large human form, as it lacks the seven Ig repeats of domain IV. More recent findings have identified a larger mouse perlecan form with three additional Ig-like repeats aligning with those of human (Noonan and Hassell, 1993).

There has also been a previous report of smaller perlecan splice variants in the worm *Caenorhabditis elegans* (Rogalski et al., 1993); the nematode homologue of perlecan, *unc-52*, undergoes alternative splicing, which results in isoforms varying in their C-terminal. The major finding of the present study is the identification of a perlecan variant, PRM, which appears to play a vital role in FGF activation during development.

Native perlecan has also recently been shown to bind FGF-2 (Aviezer et al., 1994) and it is possible that perlecan isoforms are differentially glycosylated in a manner such that particular FGFs are activated. Perlecan is a large molecule from which multiple species of proteoglycan could easily be derived either by proteolytic processing or differential exon usage. Taken together, results obtained from genomic Southern blotting demonstrate a single gene and indicate that PRM is a splice variant of perlecan. This supports previous findings from chromosomal mapping studies that assigned a single perlecan gene to mouse chromosome 4 and human chromosome I (Chakravarti et al., 1991; Cohen et al., 1993). Both the amino acid sequencing and subsequent northern and Southern analysis confirmed that the PRM molecule is related to perlecan and is clearly distinct from the syndecan HSPG family by virtue of its size distribution and profile. This was important

to establish as syndecans have been suggested to be a major regulator of FGF activation in the developing embryo (Bernfield and Hooper, 1991; Kato et al., 1994).

Numerous reports of protein isoforms of perlecan have been documented and it appears proteolytic processing of a large precursor product results in smaller forms (Klein et al., 1988; Ledbetter et al., 1985; Hassell et al., 1985). The prototypical EHS tumour-derived form of perlecan has a core of 400 kDa and three HS-side chains of 65 kDa (Noonan and Hassell, 1993). The core protein is divided into a trypsin-sensitive domain, containing the HS side chains and a trypsin-resistant domain, P200, containing two V8 protease-resistant regions of 44 kDa (P44) and 46 kDa (P46) (Ledbetter et al., 1987). Smaller perlecan isoforms with core proteins of 95-130 kDa are thought to arise from the same gene, generated proteolytically from the large 400 kDa HSPG (Kanwar et al., 1984). Such proteolytic processing of perlecan is thought to occur in various tissues; for example, although renal glomeruli express the large 400 kDa core protein of perlecan, a smaller core protein of 250 kDa of the high density proteoglycan predominates in isolated glomerular basement membrane (Klein et al., 1988). Another interesting finding from this study was the detection of secreted perlecan glycoproteins of 150-200 kDa in size, lacking HS side chains and which may have distinct functional roles. Clearly smaller perlecan isoforms may result from post-translational proteolytic processing as well from distinct mRNA variants.

In the present study, investigation of perlecan protein variants involved the isolation of proteoglycans by ion exchange chromatography from 2.3D neuroepithelial cell conditioned media. Immunoblotting using anti-perlecan polyclonal antibodies detected four different core protein variants; the native perlecan core protein of 400 kDa and core proteins of 58 kDa, 45 kDa (the core protein of PRM) and 35 kDa. Of these, only the native perlecan of 400 kDa and the smaller variant species with a core protein of 58 kDa reacted with anti-perlecan monoclonal antibodies. The results indicated that polyclonal antibodies to perlecan cross-react with PRM, but monoclonal antibodies against perlecan do not. However, the polyclonal anti-perlecan antibodies showed markedly decreased immunoreactivity to the intact PRM species of 290 kDa, compared to native perlecan species. The reduction of staining may be due to steric hindrance by HS chains present on the intact PRM molecule. It should be noted that the polyclonal anti-perlecan antibodies were not originally made against the HS side chain-containing whole proteoglycan molecule, but only the stripped core protein, which has amino acid homology to PRM. Therefore, it is not surprising that some degree of cross-reactivity was observed, strongly suggesting that perlecan and PRM share common antigenic determinants.

Polyclonal antibodies against PRM, in contrast, reacted with only the 45 kDa core protein and detected its corresponding glycosylated intact form of 290 kDa, which resolved as a sharp band on

blots. The characteristic smear often associated with heavily glycosylated proteins was not evident and may possibly be due to the self-aggregation properties of PRM. It has been suggested that proteoglycans, such as the high density proteoglycan, occur as dimers, where core proteins are attached to each other via HS-side chains (Parthasarathy and Spiro, 1982). PRM may exist as a dimer or trimer, as heparitinase treatment of the 290 kDa glycosylated form results in relatively high amounts of a single 45 kDa protein core.

There was an apparent reduction in reactivity of the anti-PRM polyclonal antibodies to the core protein of 45 kDa. Therefore, as heparanase III treatment of the PRM molecule altered immunoreactivity, it suggests that a high proportion of the polyclonal anti-PRM antibodies are directed at the heparan sulfate side chains of the molecule. Anti-PRM antibodies did not cross-react with perlecan, or any other perlecan variants present in the 2.3D cell line media, suggesting that the majority of the antigenic determinants of the anti-PRM antibodies are absent in perlecan. This result may be explained by the differ-

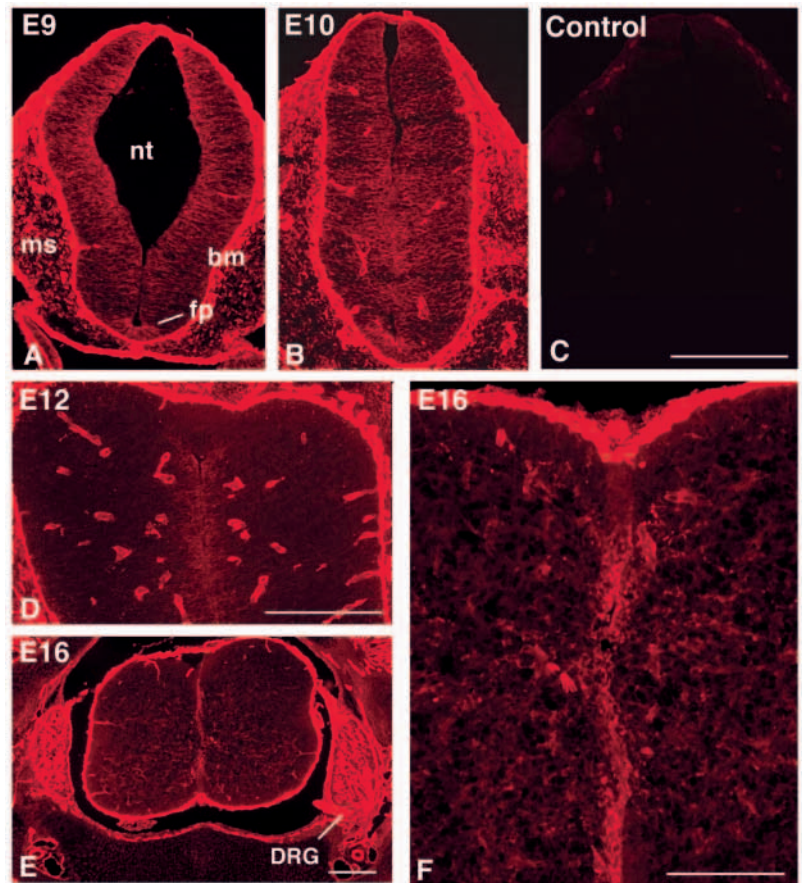


Fig. 8. Micrographs of horizontal sections through spinal cord at high cervical levels of E9 (A), E10 (B), control (C), E12 (D), E16 (E) and higher magnification of E16 spinal cord (F). All the sections were stained with the PRM-specific polyclonal antibody visible in red (Cy3) fluorescence. At E9 (A) and E10 (B) the neuroepithelial cells within the neural tube (nt) are stained, the floor plate (fp) as well as the basement membrane (bm) and mesoderm (ms). The control (C) indicates minimum background from secondary antibody. At E12 (D) and E16 (E), PRM immunoreactivity is restricted in the neuroepithelium to cells lining the lumen, as also visualised at higher magnification of E16 spinal cord (F). The dorsal root ganglia (DRG) at E16 (E) are also heavily stained. Scale bar, 100 μ m.

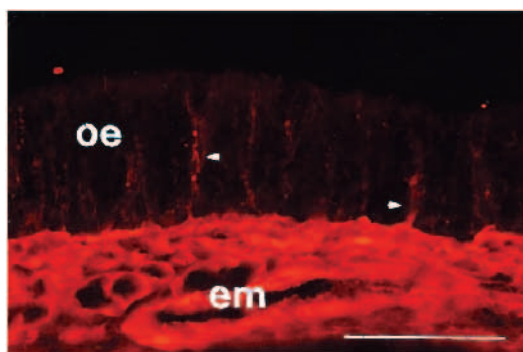


Fig. 9. Micrograph of a horizontal section through the olfactory region of a E16 mouse embryo stained for PRM immunoreactivity. In the olfactory epithelium (oe), process-like structures extending from the basement membrane towards the epithelial surface are labelled by the anti-PRM antibody (arrowheads). The extracellular matrix (em) is strongly stained. Scale bar, 50 μ m.

ences in glycosylation distribution between PRM and perlecan. The N-terminus of the large perlecan core protein contains three GAG side chains, whereas PRM appears to have several GAG side chains throughout its relatively smaller core protein (Nurcombe et al., 1993). Hence, the PRM antibodies appear to recognise heparan sulfate regions unique to PRM. Analysis of the sizes of HS chains from PRM and perlecan indicate considerable differences; the average sidechain from PRM is between 20 and 30 kDa (Nurcombe et al., 1993 and unpublished observations), whereas perlecan has sidechains between 60 and 70 kDa (Kallunki and Tryggvason, 1992).

Immunohistochemical studies using the perlecan monoclonal antibody and PRM polyclonal antibodies revealed perlecan staining in the basement membrane and surrounding mesoderm of E10 mouse spinal cord. PRM, however, showed additional and unique expression in the neuroepithelial cells of the spinal cord. This pattern of staining extended into the telencephalic vesicles of the neural tube. This result supports previous studies from our laboratory, which demonstrated the colocalisation of FGF-2 and the novel HSPG-PRM within the proliferating precursor population of the neuroepithelium (Ford et al., 1994). The immunostaining revealed colocalisation of FGF-2 with that of the HSPG on the surface of cell bodies in the neuroepithelium, strongly suggesting a functional interaction. In contrast to the pattern observed in the neural tube, the present study revealed colocalisation of PRM and perlecan within the neural precursor cells of the otic vesicle. These cells are not derived from the neural tube, but arise from an otic placode which itself is derived from the surface ectoderm. It is thus possible that these different neural lineages may utilise perlecan variants for different functions. By E16 the number of proliferating ventricular precursor cells in the mouse has markedly declined. At this later stage, PRM was found to be restricted to the still proliferating subventricular region of the lateral and fourth ventricle, consistent with a role in precursor proliferation. Once again, perlecan expression was not detectable in this region.

The localisation of perlecan in this present study is in agreement with past findings. Previous reports of immunoenzymatic staining of perlecan has located it to the basement membranes of all tissues, including all vascular basement

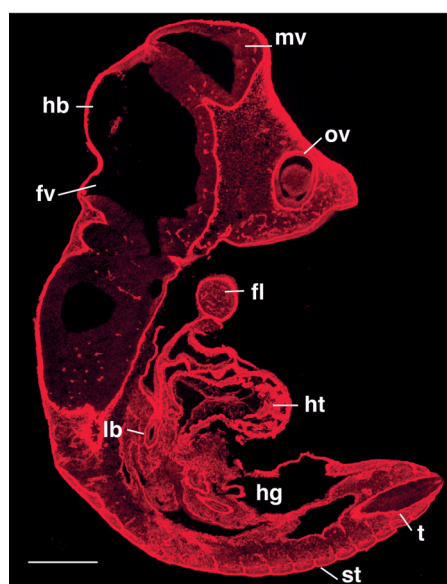


Fig. 10. Low power micrograph of a sagittal section through an E10 mouse embryo stained for PRM immunoreactivity. ECM and basement membrane of most tissues are strongly labelled. The nervous system reveals staining in the basement membrane and neuroepithelium of the mesencephalic (mv) and fourth ventricle (fv), staining of individual neuroepithelial cells can not be visualised at this magnification. The dorsal aspects of somites (st) of the spinal cord are stained. In the tail (t) region, PRM immunoreactivity is visible towards the lumen of the spinal cord. The eye capsule of the optic vesicle (ov) is stained intensely. The basement membranes and mesenchyme of the forelimb(fl), lung bud (lb) and hind gut (hg) are also intensely stained. In addition the PRM is heavily localised to the vascular system, especially the heart (ht). Scale bar, 500 μ m.

membranes and those at epithelial and mesenchymal interfaces (Dziadek et al., 1985; Murdoch et al., 1994). Perlecan is not exclusively confined to basement membranes, but is also found in stromal elements of connective tissue, and sinusoidal vessels of liver, spleen, lymph nodes and pituitary gland (Couchman and Ljubimov, 1989). In this study, perlecan protein was not found surrounding individual neuroepithelial cells, although the 2.3D neuroepithelial cell line was shown to express perlecan mRNA. In addition, PCR studies on E10 neuroepithelial tissue also indicated the presence of perlecan mRNA transcripts (S. Joseph and U. Greferath, unpublished observations). A number of epithelial and mesenchymal cell types have been shown to express the perlecan message; for example, both colon carcinoma and fibroblast cells express the perlecan transcript (Murdoch et al., 1994).

The localisation of PRM in the developing mouse spinal cord revealed staining of neuroepithelial cells at E9 and E10, whereas at E12 and E16 only residual precursor cells lining the central lumen were positive for PRM. Intense staining of the floor plate was observed at E9, this active domain of neuroepithelial cells gives rise to the neural tube and entire central nervous system which further indicates the significance of PRM in early neural development. The developing notochord, which induces the overlying ectoderm to thicken and form the floor plate, is also heavily stained for PRM. The sensory neurons of the dorsal root ganglion strongly express PRM by E16. At E16, immunostaining for PRM could be seen in the

ECM of the olfactory system, and extending into the olfactory epithelium; this is particularly interesting as this epithelium continues to divide throughout adult life. The staining pattern within the epithelial layer is similar to staining that revealed the pattern of ingrowth of developing trigeminal nerve fibres (Finger and Bottger, 1993), fibres known to respond to FGFs.

PRM was not only localised to the developing nervous system but was shown to have a ubiquitous expression throughout the developing embryo. The pattern of PRM staining in sagittal sections of whole E10 embryos reveals strong staining to the ECM and basement membrane of various tissues, as well as staining structures derived from mesenchyme, endoderm and ectoderm. Analysis of the nervous system as seen in this section revealed staining in the basement membrane and neuroepithelium of the mesencephalic and fourth ventricle. All of neuroepithelial tissue at this stage of development are undergoing rapid mitosis and PRM might thus be expected to be present. In addition the somites adjacent to the spinal cord are stained, particularly towards their dorsal aspect, which probably reflects the neural crest-derived dorsal root ganglia. The neural tube in tail bud region is viewed in transverse section and indicates strong PRM localisation to the neuroepithelial cells of the neural lumen. The eye capsule also stains intensely with PRM. This optic cup is an outgrowth of the neuroectoderm of the forebrain and its inner layer proliferates to form a thick neuroepithelium, which later differentiates into the retina. PRM intensely stained the basement membrane and various structures of mesodermal and endodermal origin. For instance, the limb bud, which elongates through the proliferation of mesenchyme, stained with PRM, as did the lung bud, which is of endodermal origin. PRM was also localised to the growing mesenchyme of the face and nasal region, as well as, the developing embryonic gut which is composed of both endoderm and mesoderm. PRM is heavily localised to the vascular system especially the heart and blood vessels which are of mesenchymal origin and are supported by a basement membrane.

In summary, our immunohistochemical results suggest that PRM shows a markedly different expression pattern to perlecan; wherein the PRM molecule is uniquely found on the surface of neuroepithelial cells and in mesenchymal and endodermal tissue of the developing embryo. The PRM molecule also appears to be distinct to native perlecan, as it seems to harbour unique heparan sulfate side chains due to differential glycosylation of the core protein. Our studies suggest that PRM is an alternative splice variant of perlecan and therefore encoded by the same gene. Definitive characterisation of HSPG-PRM awaits the completion of cloning and sequencing of the molecule. Further studies are in progress to establish whether PRM is continually expressed into adulthood in various tissues. Preliminary results indicate a ubiquitous pattern of PRM staining in the ECM and blood vessels of various adult tissues (S. Joseph, unpublished observations). Our results are consistent with the hypothesis that this novel HSPG is a variant of perlecan that is highly expressed in early neural tissue to perform a specific role in early growth and differentiation by regulating cellular responses to FGFs.

We are grateful to Dr Marie Dziadek for providing polyclonal antibodies to perlecan and Dr Merton Bernfield for Syndecan cDNA probes. We thank also members of Dr Alan Snow's laboratory at the University of Washington and Adam Puche for helpful discussions.

This work was supported from the National Health and Medical Research Council of Australia, funding from AMRAD Australia, and funding from the *Deutsche Forschungsgemeinschaft*, Germany.

REFERENCES

- Aviezer, D., Hecht, D., Safran, M., Elsinger, M., David, G. and Yayon, A. (1994). Perlecan, basal lamina proteoglycan, promotes basic FGF-receptor binding, mitogenesis and angiogenesis. *Cell* **79**, 1005-1013.
- Bernfield, M. and Hooper, K. C. (1991). Possible regulation of FGF activity by Syndecan, an integral membrane heparan sulfate proteoglycan. *Annals NY Acad. Sci.* **638**, 182-194.
- Carey, D. J., Evans, D. M., Stahl, R. C., Asund, U. K., Conner, K. J., Garbes, S. P. and Cizmeci, S. G. (1992). Molecular cloning and characterisation of N-Syndecan, a novel transmembrane heparan sulfate proteoglycan. *J. Cell Biol.* **117**, 191-201.
- Chakravarti, S., Phillips, S. L. and Hassell, J. R. (1991). Assignment of perlecan (heparan sulfate proteoglycan) gene to mouse chromosome 4. *Mamm. Genome* **1**, 270-272.
- Chu, G., Vollrath, D. and Davis, R. W. (1986). Separation of large DNA molecules by contour-clamped homogenous electric fields. *Science* **234**, 1582-1585.
- Cohen, I. R., Grassels, S., Murdoch, A. D. and Iozzo, R. V. (1993). Structural characterisation of the complete human perlecan gene and its promoter. *Proc. Natl. Acad. Sci. USA* **90**, 10404-10408.
- Couchman, J. R. and Ljubimov, A. V. (1989). Mammalian tissue distribution of a large heparan sulfate proteoglycan detected by monoclonal antibodies. *Matrix* **9**, 311-321.
- David, G. (1991). Biology and pathology of the pericellular heparan sulfate proteoglycans. *Biochemical Society Transactions* **19**, 816-820.
- Dziadek, M., Fujiwara, S., Paulsson, M. and Timpl, R. (1985). Immunological characterisation of basement membrane types of heparan sulfate proteoglycans. *EMBO J.* **4**, 905-912.
- Finger, T. E. and Bottger, B. (1993). Peripheral peptidergic fibres of the trigeminal nerve in the olfactory bulb of the rat. *J. Comp. Neurol.* **334**, 117-124.
- Ford, M. D., Bartlett, P. F. and Nurcombe, V. (1994). Co-localisation of FGF-2 and a novel heparan sulphate proteoglycan in embryonic mouse brain. *NeuroReport* **5**, 565-568.
- Gallagher, J. J. and Turnbull, J. E. (1992). Heparan sulphates in the binding and activation of bFGF. *Glycobiology*, **2**, 523-528.
- Greferath, U., Grunert, U. and Wassele, H. (1990). Rod bipolar cells in the mammalian retina show protein kinase C-like immunoreactivity. *J. Comp. Neurol.* **301**, 433-442.
- Hassell, J. R., Keyshon, W. C., Ledbetter, S. R., Tyree, B., Suzuki, S., Kato, M., Kimata, K. and Kleinman, H. K. (1985). Isolation of two forms of basement membrane proteoglycans. *J. Biol. Chem.* **260**, 17668-17676.
- Hassell, J. R., Robey, P. G., Barrach, H. J., Wilczek, J., Rennard, S. I. and Martin, G. R. (1980). Isolation of HS-containing proteoglycans from basement membrane. *Proc. Natl. Acad. Sci. USA* **77**, 4494-4498.
- Iozzo, R. V. and Wight, T. N. (1982). Isolation and characterisation of proteoglycans synthesized by human colon and colon carcinoma. *J. Biol. Chem.* **257**, 11135-11144.
- Iozzo, R. V. and Hassell, J. R. (1989). Identification of the precursor protein for the heparan sulfate proteoglycan of human colon carcinoma cells and its post-translational modifications. *Arch. Biochem. Biophys.* **269**, 239-249.
- Iozzo, R. V., Cohen, I. R., Grassel, S. and Murdoch, A. D. (1994). The biology of perlecan, the multifaceted heparan sulphate proteoglycan of basement membranes and pericellular matrices. *Biochem. J.* **302**, 625-639.
- Kallunki, P. and Tryggvason, K. (1992). Human basement membrane heparan sulfate proteoglycan core protein: a 467 kDa protein containing multiple domains resembling elements of the low density lipoprotein receptor, laminin, neural cell adhesion molecules and epidermal growth factor. *J. Cell Biol.* **116**, 559-571.
- Kanwar, Y. S., Veis, A., Kimura, J. H. and Jakubowski, M. L. (1984). Characterization of heparan sulfate-proteoglycan of glomerular basement membranes. *Proc. Natl. Acad. Sci. USA* **81**, 762-766.
- Kato, M., Wang, H., Bernfield, M., Gallagher, J. J. and Turnbull, J. E. (1994). Cell surface Syndecan-1 on distinct cell types differs in fine structure and ligand binding of its heparan sulfate chains. *J. Biol. Chem.* **269**, 18881-18890.

- Kjellen, L. and Lindahl, V.** (1991). Proteoglycans: Structures and interactions. *Ann. Rev. Biochem.* **60**, 443-475.
- Klein, D. J., Brown, D. M., Oegema, T. R., Brenchley, P. E., Anderson, J. E., Dickinson, M. A., Horigan, E. A. and Hassell, J. R.** (1988). Glomerular basement membrane proteoglycans are derived from a large precursor. *J. Cell Biol.* **106**, 963-970.
- Ledbetter, S. R., Tyree, B., Hassell, J. R. and Horigan, E. A.** (1985). Identification of the precursor protein to basement membrane heparan sulfate proteoglycans. *J. Biol. Chem.* **260**, 8098-8105.
- Ledbetter, S. R., Fisher, L. W. and Hassell, J. R.** (1987). Domain structure of the basement membrane heparan sulfate proteoglycan. *Biochemistry* **26**, 988-995.
- Murdoch, A. D. and Iozzo, R. V.** (1993). Perlecan: the multidomain heparan sulphate proteoglycan of basement membrane and extracellular matrix. *Virchows Archiv Pathol. Anat.* **423**, 237-242.
- Murdoch, A. D., Liu, B., Schwarting, R. and Tuan, R. S.** (1994). Widespread expression of perlecan proteoglycan in basement membranes and extracellular matrices of human tissue as detected by a novel monoclonal antibody against domain III and by *in situ* hybridization. *J. Histochem. Cytochem.* **42**, 239-249.
- Noonan, D. M., Horigan, E. A., Ledbetter, S. R., Vogeli, G., Sasaki, M., Yamada, Y. and Hassell, J. R.** (1988). Identification of cDNA clones encoding different Domains of the basement membrane heparan sulfate proteoglycan. *J. Biol. Chem.* **263**, 16379-16387.
- Noonan, D. M., Fulle, A., Valente, P., Cai, S. J., Horigan, E., Sasaki, M., Yamada, Y. and Hassell, J. R.** (1991). The complete sequences of perlecan, a basement membrane heparan sulfate proteoglycan, reveals extensive similarity with laminin alpha chain, low density lipo-protein receptor and the neural cell adhesion molecule. *J. Biol. Chem.* **266**, 22939-22947.
- Noonan, D. M. and Hassell, J. R.** (1993). Perlecan, the large low-density proteoglycan of basement membranes: structure and variant forms. *Kidney Int.* **43**, 53-60.
- Nurcombe, V., Ford, M. D., Wildschut, P. F. and Bartlett, P.** (1993). Developmental regulation of neural response to FGF-1 and FGF-2 by heparan sulfate proteoglycan. *Science* **260**, 103-106.
- Parthasaty, N. and Spiro, R. G.** (1984). Isolation and characterisation of the heparan sulfate proteoglycan of the bovine glomerular basement. *J. Biol. Chem.* **259**, 12749-12755.
- Rogalski, T. M., Williams, B. D., Mullen, G. P. and Moerman, D. G.** (1993). The products of the *unc-52* gene in *Caenorhabditis elegans* are homologous to the core protein of the mammalian basement membrane heparan sulfate proteoglycan. *Genes and Development* **7**, 1471-1484.
- Rohrbach, D. H., Hassel, J. R., Kleinman, H. K. and Martin, G. R.** (1982). Alterations in the basement membrane (heparan sulfate) proteoglycan in diabetic mice. *Diabetes* **31**, 185-188.
- Rohrbach, D. H., Wagner, C. W., Star, V. L., Martin, G. R., Brown, K. S. and Yoon, J. W.** (1983). Reduced synthesis of basement membrane heparan sulfate proteoglycan in streptozotocin-induced diabetic mice. *J. Biol. Chem.* **258**, 11672-11677.
- Ruoslahti, E. and Yamaguchi, Y.** (1991). Proteoglycans as modulators of growth factor activities. *Cell* **64**, 867-869.
- Saunders, S., Jalkanen, M., O'Favel, S. and Bernfield, M.** (1989). Molecular cloning of Syndecan, an integral membrane proteoglycan. *J. Cell Biol.* **108**, 1547-1556.
- Snow, A. D., Wight, T. N. and Prusiner, S. B.** (1989). Proteoglycans in the pathogenesis of Alzheimer's disease and other amyloidoses. *Neurobiol. Aging* **10**, 481-497.
- Vihinen, T., Auvinen, P., Alanen-Kurki, L. and Jalkanen, M.** (1993). Structural organization and genomic sequence of mouse syndecan-1 gene. *J. Biol. Chem.* **268**, 17261-17269.
- Wang, F., Kan, M., Xu, J., Yan, G. and McKeehan, W. L.** (1995). Ligand-specific structural domains in the fibroblast growth factor receptor. *J. Biol. Chem.* **270**, 10222-10230.
- Wight, T. N., Kinsella, M. G. and Qwarnstrom, E. E.** (1992). The role of proteoglycans in cell adhesion, migration and proliferation. *Curr. Opin. Cell Biol.* **4**, 793-801.
- Yurchenco, P. D., Cheng, V. S. and Ruben, G. C.** (1987). Self-assembly of a high molecular weight basement membrane heparan sulfate proteoglycan into dimers and oligomers. *J. Biol. Chem.* **262**, 17668-17676.
- Yurchenco, P. D. and Schittny, J. C.** (1990). Molecular architecture of basement membranes. *FASEB J.* **4**, 1577-1590.